A VIBRATING DIAPHRAGM PRESSURE MEASURING SYSTEM

J. Dimeff
Chief, Instrumentation Division
J. W. Lane
Research Scientist
G. J. Deboo
Research Scientist
R. C. Hedlund
Research Scientist
Ames Research Center, NASA
Moffett Field, Calif. 94035

ABSTRACT

A system has been developed that will measure pressure over the range 10^{-5} to 4×10^{3} Torr in a rugged, lightweight package suitable for airborne and space applications. It consists of a transducer which measures pressure by sensing the damping of a vibrating diaphragm immersed in the gas, and the electronics necessary to drive the transducer and supply data to a recorder or telemetry. The system has been used on prototype atmosphere entry probes to define a planetary atmosphere profile. The operation of the system is described and data on its performance are presented.

INTRODUCTION

A novel tranducer developed to measure pressure in the wind tunnels of Ames Research Center is described in references 1 and 2. This transducer measures pressure over a wide range by sensing the power required to maintain the resonant vibration of a thin metallic membrane that is immersed in a test gas and placed between two stationary plates as shown in figure 1. The power required to maintain the oscillation in the presence of viscous damping losses introduced by the gas is derived from an electrostatic voltage applied to the stationary forcing plate. The displacement of the moving membrane is sensed by measuring the capacitance variation between the membrane and the stationary sensing plate.

An appropriate set of electronics designed for the transducer, and which will be discussed below in considerable detail, is shown in figure 2. The periodic change in capacitance due to diaphragm motion is measured and converted to an electrostatic forcing voltage at a level adequate to maintain the desired amplitude. This forcing voltage is related to the gas damping and provides a measure of the gas pressure from approximately 10^{-5} to 5×10^{3} Torr, with an accuracy of better than 1 percent of reading over much of this range.

The device overcomes many of the shortcomings of other pressure gages: it is small and rugged; it has an unusually wide dynamic range; it lends itself readily to automatic operation; it is characterized by an error proportional to the pressure being measured, rather than the full scale of the instrument; it is an absolute instrument requiring no reference pressure; and it has a relatively fast response time.

These advantages suggest that the transducer would be an excellent choice for use on an experiment to determine the pressure-altitude distribution for the atmosphere of a planet such as Mars. The special requirements of such an application have led to a review of the mechanical design and of the design of the electronics associated with the transducer.

The range of the vibrating diaphragm transducer is partly limited by the energy loss inherent to the diaphragm. The energy dissipated by the periodic motion of the gas is reduced as the gas pressure is reduced until it is equal in magnitude to the energy lost within the diaphragm as a result of the inelastic deformation of the metal. Such unwanted losses can be caused either by stress concentrations near the edge of the diaphragm where it is attached to the body of the transducer by spot welding, or by viscoelastic losses due to the periodic stress applied to the diaphragm. At pressures significantly lower than this value, use of the transducer requires measurement of a small gas effect in the presence of relatively large losses in the metal diaphragm. The range of the transducer is limited when the viscous losses associated with the gas at high pressures become so great that a condition of resonance can no longer be said to exist.

The main body of this paper will be devoted to a discussion of the techniques being utilized to reduce the importance of these limitations, a discussion of the electronics required to make the system operate over a range of many decades, and a description of the performance characteristics associated with the current flight prototype.

NEW TECHNIQUES

Dimeff, Lane, and Coon[1] have analyzed the transducer configuration shown in figure 3, and derived the following expression for the electrostatic power required to move the membrane:

$$P_e = \frac{\pi r_p^{\,2} \varepsilon V_S V_V A_o \omega}{2X_p^{\,2}} \qquad (1)$$

where r_p is the radius of the driving plate, ε is the dielectric constant for the gas, V_S is the dc bias voltage, V_V is the amplitude of the applied sinusoidal voltage, A_o is the peak

16 p) none

TMX-66384

displacement of the diaphragm averaged over the area of the fixed plate, X_p is the spacing between the diaphragm at rest and the fixed plate, and ω is the resonant frequency of the diaphragm in radians per second. The analysis assumes small displacements and symmetry of construction with respect to the forcing and sensing sides of the transducer. Equations relating the forcing voltages to the pressure being measured were also derived. For the low pressure region where the mean free path is large compared with the dimensions of the transducer,

$$\frac{V_s V_v}{A_o} = \frac{32\beta\bar{c}X_p^{\,2}}{\varepsilon\omega r_p^{\,2}} \left\{ 1 - \frac{\begin{pmatrix} 16[\mathrm{ber}(\alpha R_o)\mathrm{ber}'(\alpha R_o) \\ + \mathrm{bei}(\alpha R_o)\mathrm{bei}'(\alpha R_o)] \end{pmatrix}}{\begin{pmatrix} \alpha^3 R_o^{\,3}[\mathrm{ber}^2(\alpha R_o) \\ + \mathrm{bei}^2(\alpha R_o)] \end{pmatrix}} \right\} P_o \qquad (2)$$

For higher pressures

$$\frac{V_s V_v}{A_o} = \frac{16X_p^{\,3}}{9\varepsilon\mu r_p^{\,2}\omega} \left\{ 1 - \frac{\begin{pmatrix} 16[\mathrm{ber}(\alpha R_o)\mathrm{ber}'(\alpha R_o) \\ + \mathrm{bei}(\alpha R_o)\mathrm{bei}'(\alpha R_o)] \end{pmatrix}}{\begin{pmatrix} \alpha^3 R_o^{\,3}[\mathrm{ber}^2(\alpha R_o) \\ + \mathrm{bei}^2(\alpha R_o)] \end{pmatrix}} \right\} P_o \qquad (3)$$

where β is the momentum transfer accommodation coefficient, which is approximately equal to unity for air, $\bar{c}$ is the mean molecular velocity of the gas, μ is the coefficient of viscosity, R_o is the diaphragm radius, P_o is the pressure being measured, and α is the mean free path of the gas and is given by the expression

$$\alpha = \left\{ \frac{\mu\omega}{[3\beta\lambda X_p + (X_p^{\,2}/9)]P_o} \right\}^{1/2}$$

Fortunately, for the configuration considered in figure 3, the spacings and natural resonant frequencies were such that good approximations could be used, and Eqs. (2) and (3) could be reduced to the much more useful forms

$$\frac{V_s V_v}{A_o} = \frac{32}{\varepsilon} \frac{\beta\bar{c}}{\omega} \frac{X_p^{\,2}}{r_p^{\,2}} P_o \qquad (4)$$

and

$$\frac{V_s V_v}{A_o} = \frac{16X_p^{\,3}}{9\varepsilon\mu r_p^{\,2}\omega} P_o^{\,2} \qquad (5)$$

It should be noted that for the very low pressure regime ($P_o < 10^{-4}$ Torr), Eq. (4) is not valid since it does not consider internal losses associated with the diaphragm. These losses of course ultimately limit the resolution of the transducer. A more accurate equation for this low pressure region is

$$P_e = P_{gas} + P_{int} \qquad (6)$$

where P_{gas} is the power dissipated through viscous gas losses and P_{int} is power dissipated internally by the diaphragm. It then follows from Eqs. (1) and (4) that

$$P_e = 16\Pi \frac{\beta\bar{c}}{\varepsilon} A_o^{\,2} P_o + P_{int} \qquad (7)$$

The most conventional measure of the internal loss for a system is the Q, defined as $2\Pi(W/\Delta W)$ where ΔW is the energy loss per cycle and W is the maximum energy of the system. Using this definition for Q and noting that $W = (\rho/2)\pi r_p^{\,2} d A_o^{\,2}\omega^2$, Eq. (7) may be written as follows:

$$Q^{-1} = \frac{32\pi\beta\bar{c}}{M\omega^3} P_o + Q_{int}^{-1} \qquad (8)$$

where d is the membrane thickness, ρ is the membrane density, and M is the membrane mass. If Eq. (8) is evaluated for the transducer shown in figure 1 at a pressure 10^{-5} Torr, the magnitude of the first term on the right side of the equation is $Q_{gas}^{-1} = 1.3\times10^{-6}$ which indicates that ideally Q should equal 770,000. Unfortunately, at this pressure the measured value of Q was typically 15,000 for the original generation of transducers and particularly good transducers had Q's as high as 30,000.

An investigation with respect to these important internal losses is currently being undertaken at Ames Research Center, but the theoretical aspects of this program will not be reported at this time. For the interested reader, references 3, 4, and 5 contain a good survey of the internal losses arising from thermoelastic effects, point defects, and dislocation phenomena. A comprehensive survey of the literature in this field tends to indicate that a great deal of work remains to be completed before really quantitative predictions can be made with respect to minimizing membrane losses by the proper choice of materials, heat treatment, cold work, and mounting techniques. Results experienced with heat treatment of the tranducers, however, suggest that one should be able to obtain diaphragms routinely with Q's greater than 50,000. In one case we were able to anneal a tensioned diaphragm mounted to its cell body at 960° F in nitrogen for 1/2 hour and obtain a resultant Q of 250,000 measured at 10^{-5} Torr. Experiments with heat treatment and welding techniques are being continued.

Extending the pressure measurement range at high pressures involves a completely different set of problems. The vibrating diaphragm transducer in figure 3 suffers from several disadvantages derived from its basic design. The spacing between the moving diaphragm and the fixed forcing and sensing plates is small, so that the moving membrane does substantial work on the gas being measured. Unfortunately, with this geometry, the damping increases with increasing pressure more rapidly than is desirable at higher pressures so that because of low effective Q, the sensor ceases to function as

a simple mechanical resonant system and is incapable of measuring pressure in the range above 1000 Torr. Since the effective stiffness also increases with pressure because of the periodic volume change of each gas chamber, the resonant frequency of the system changes radically at pressures above approximately 100 Torr. This change in frequency causes the mechanical frequency of the diaphragm, due to gas stiffness, to overlap an acoustic resonance associated with the interior dimensions of the transducer body. These problems have been minimized by the transducer configuration in figure 4. The performance of the device has been significantly improved as a result of the grid-damping plate structure. The functions of the forcing plate and sensing plate have now been taken over by forcing and sensing grids which are maintained at close proximity to the membrane while the solid plates that control the stiffness introduced by the gas are moved farther from the membrane. The advantage of this configuration is that the designer has considerable freedom in choosing the interior transducer geometry without sacrificing effective driving force or displacement sensing sensitivity. A quantitative theoretical analysis of this transducer has not been completed because of the relatively limited amount of time thus far devoted to it.

Before describing the mechanical design of the transducer in more detail, it is perhaps worthwhile to digress for a moment in order to discuss another transducer modification that has been incorporated in the grid cell configuration. The area of the grids has been very carefully chosen to suppress the sensing of higher modes of resonant vibration. The diaphragm displacement is described by Bessel functions for which the radially symmetrical modes of vibration are

$$y_n(r,t) = A_{on} J_{on}\left(X_n \frac{r}{R_o}\right) \cos 2\pi f_n t \qquad (9)$$

where r is the radial distance from the center of the diaphragm, t is time, X_n is the nth root of $J_o(X) = 0$, and A_{on} is the displacement amplitude. It then follows that the average displacement of the membrane is given by

$$\left.\begin{aligned} \bar{y} &= \int_o^{R_p} \frac{A_{on}}{\pi R_p^2} J_{on}\left(X_n \frac{r}{R_o}\right) \cos 2\pi f_n t (2\pi r)\,dr \\ \bar{y} &= \frac{A_{on} R_o}{\pi R_p X_n} \cos 2\pi f_n t J_1\left(X_n \frac{R_p}{R_o}\right) \end{aligned}\right\} \qquad (10)$$

If R_p can be chosen so that $J_1[X_n(R_p/R_o)] = 0$, the dynamic capacitance change would be equal to zero and, hence, no output signal would be detected for this mode of vibration. In general then, to selectively reject signals of a particular higher mode of vibration, the radius of the sensing area should be chosen so that

$$R_p = \frac{Y_{n-1}}{X_n} R_o \qquad (11)$$

where R_p is the radius of the sensing area, R_o is the diaphragm radius, X_n is the nth root of J_o, Y_{n-1} is the n-1 root of J_1 and n the index of mode to be suppressed. For the grid transducer, our primary interest was in the suppression of the J_{02} mode which is a mode of vibration having two concentric nodes including the node at R_o, and hence, $R_p = Y_1 R_o / X_2 = 0.695\ R_o$. For this transducer the J_{21} mode is also relatively signficant. Fortunately this mode has two diametrical nodes and the motion is such that $\bar{y} = 0$ if the sensing area is concentric and parallel to the membrane. These conditions are met by the geometry designed to suppress the J_{02} mode. The effectiveness of this method of suppressing higher modes is evident from the data in table 1 for the relative strength of the higher modes in a transducer that was specifically designed for higher mode suppression and for a transducer of the original design as shown in figure 3 with normal machining tolerances.

Preliminary experiments are currently being performed with the transducer shown in figure 5. This configuration uses three commercially available hermetic feed-throughs to support each of the stationary plates. Early results of these experiments are exciting because they indicate this geometry eliminates the undesirable acoustic resonances mentioned earlier and that the frequency now continues to increase with increasing pressure. The drive voltage requirements do not differ significantly from those of the standard transducer over most of the pressure range. This frequency variation is extremely significant since it changes from approximately 5,000 Hz to 70,000 Hz over the interval from 10^{-3} Torr to 760 Torr. This large frequency variation makes this configuration particularly attractive when it is desirable to determine the pressure from frequency measurements. The data taken for the transducer are shown in figure 6. It is evident that frequency deviations as a function of temperature could cause errors for this mode of operation. However, the frequency deviation observed for the standard transducer at vacuum is approximately 0.014%/°C. Because of its construction this new configuration should be even less sensitive to temperature change and hence the problem should not be serious. This new embodiment offers a further advantage in that it is much easier to fabricate than the standard transducer configuration.

The initial grid-type transducer design shown in figure 4 is fabricated from metal-ceramic seals. The body is a 42% NiFe alloy and the ceramic insulating disc is Al_2O_3, which was chosen for a good match with respect to thermal expansion coefficient. The diaphragm material is 44% NiFe annealed at 960°F. Experience has shown this material to be more satisfactory than 42% NiFe or several other alloys that have been tested on the basis of matching the thermal expansion coefficient of the membrane to the composite coefficient of the transducer body. While under tension, the 0.0001 in. membrane is mounted to one half of the body with an overlapping spot weld. The grid structure is 0.0001 in. thick Ni having approximately 50% open area, and it is spot welded to the top of the damping

structure. The most important dimensions for the design of this configuration are shown in figure 4.

Table 1 lists the improvements that have been achieved and compares them with the results obtained with the original design shown in figure 3.

ELECTRONICS

The open-loop system for driving the pressure transducer shown in figure 1 is not convenient since both the resonant frequency of the diaphragm and the amplitude of vibration change as the pressure is varied. In order to eliminate the need for manual adjustment and achieve a time response fast enough to meet the wind-tunnel requirements, the original closed-loop system[1] and a completely electronic servo were built for wind-tunnel use. Figure 2 is a block diagram of the present system which has been modified to meet the requirements of the applications currently being considered. The numbers above the functional blocks correspond to the modules shown in the detailed sketch of the electronics, figure 7.

The circuit design was influenced by several factors, but principally by the requirement that the system be suitable for landing on planets other than Earth. For this application, the system must be sterilizable, that is, capable of being heated to 135°C for six periods of 92 hours each. Size, power, and reliability were also important factors. These requirements were met in the design shown in figures 7 and 8. A detailed description of circuit operation will not be given in this paper, but the overall system presented challenging design problems because of the dynamic range and precision of the instrument. An analysis of the tracking filter (M8 in fig. 7) will be presented in a forthcoming paper.

The operation of the system can best be understood by reference to figure 2. In this arrangement the displacement of the diaphragm causes a capacitance change, which in turn, generates an input to a velocity sensing preamplifier. The output of the preamplifier is then amplified, filtered, rectified, and compared to a pre-set dc reference voltage in the rectifier-reference module. This unit generates a dc voltage input to the drive-output module whose dc output voltage is periodically switched by the output of module 3, the chopper-drive module. Since this output is synchronized with the membrane velocity, the voltage drives the diaphragm at its resonant frequency and at an amplitude sufficiently large that the input voltage to M4 after rectification is equal to the reference voltage.

The function of each block in figure 2 may be described as follows. M1 is a preamplifier and differentiator and the cell itself is the capacitor required to affect the differentiation. This preamplifier provides the 90° phase shift necessary to provide the proper phase shift for the cell driving force. M2 is an ac amplifier with a gain of 100. M8 is a narrow band tracking filter which self-tunes to the resonant frequency of the transducer and also maintains zero phase shift from its input to output. M4 is a precision rectifier, and contains the temperature-stable dc reference. M3 converts the sine wave from M8 into the square wave necessary to drive M5. M5 provides the ac-dc electrostatic drive to the transducer as well as the system output voltage. M7 is an automatic gain switch, which reduces the open-loop gain of the system to insure stability when the cell Q changes to values above approximately 1000. M6 is a dc to dc converter and regulator which converts an input power supply voltage of approximately 28 volts to the voltages necessary to power the various modules.

The electronic unit described above controls the resonant deflection of the membrane vibration to a value established by the reference voltage and by the gain of the linear ac amplifiers. The condition actually being controlled is that ΔV (the preamplifier output voltage) be constant, independent of the pressure being measured. It can be shown that the following expression is valid for the preamplifier:

$$\frac{\Delta V}{V_{bias}} = K_1 \frac{\Delta C}{C_o} \frac{\omega}{\omega_o} = K_2 A_o \frac{\omega}{\omega_o} \tag{12}$$

where ΔC is the detected change in capacitance; C_o is the rest capacitance of the transducer; A_o is the amplitude of the diaphragm motion; ω_o is the frequency of the transducer at high vacuum; ω is the frequency at the pressure being measured; and K_1 and K_2 are constants. It then follows that the controlling condition in the loop requires that $A_o\omega$ be held constant. Eq. (4) establishes that for a wide range of pressures,

$$\frac{V_S V_V}{A_o} = K_3 P_o \tag{13}$$

where P_o is the pressure being measured, and K_3 is a constant. For the circuit of figures 2 and 6, V_S and V_V are both derived from the dc output of the rectifier-reference module and are linearly related. Eq. (13) may therefore be written in the form $V_S^2 = KP_o/\omega$. It is worth noting that in addition to this square law dependence, the system readily lends itself to operation in either a mode where the pressure is proportional to the first or third power of the voltage. For example, if V_S were held constant and equal to V_{bias}. It can be seen from Eq. (13) that V_V would be linearly related to the pressure. V_{bias} may also be equal to V_S, thereby being changed as the pressure is varied. For this mode of operation, A_o then also varies with pressure, and from the arguments given above, it can be shown that $V_S^3 = KP_o/\omega$.

SYSTEM PERFORMANCE

A comprehensive discussion of a technique for determining the properties of planetary atmospheres is given in references 6 and 7. The technique is based on measurements of temperature, pressure, and acceleration during free-fall through the atmosphere. An early version of the vibrating

diaphragm system was used to provide pressure measurements on these Earth atmosphere experiments. The system after impact was completely operational. The system also satisfied a series of rigid preflight requirements including sinusoidal vibration at a level of ±10 g along all axes over the interval from 0-2000 Hz and static acceleration at 50 g. The transducer was sterilized at 135°C for three, 8-hour intervals with no observable degradation in performance. It also survived a drop test of 250 g parallel to the membrane. The pressure measurement range required for the atmospheric entry experiments was limited to the interval from approximately 1 Torr to 200 Torr.

Figure 8 is a photograph of the current space flight prototype scheduled for use on a rocket-launched vehicle containing a comprehensive series of atmospheric composition experiments. Since these particular tests require pressure measurements over only a limited range, either the standard or grid-type transducer configuration is adequate for the experiment. The reproducibility of measurements made with the original pressure transducer over its complete range is shown by the solid line in figure 9. The repeatibility of the present prototype system with a standard cell over the limited portion of the range required for the rocket experiment is shown by the data points in that figure. It should be remembered that the fractional standard deviation shows the error based on the pressure being measured rather than full-scale pressure, and that a 3σ deviation (where σ is the standard deviation) indicates a confidence level of 99.7%. The performance of a breadboard model of the system with a grid-type transducer is shown in figure 10. The flight prototype unit weighs approximately 12 ounces, has a volume of approximately 8 cubic inches, requires 0.650 watts of power, and has a time response of approximately 0.050 sec.

FUTURE APPLICATIONS

This system has been developed to meet the needs of experiments in the atmospheres of the planets. The direct results of the development, however, suggest applications in altimetry, meteorology, and laboratory instrumentation where extremely wide dynamic range, absence of zero drift, freedom from the hazard of pressure overload damage, small sampling volume, ruggedness, and small size would offer clear advantages. The indirect results of these developments suggest the possibility of significant improvements in the performance of those transducers used in electrometers, radiometers, and other areas where the sensing action depends on a resonant mechanical member.

KEY WORDS

Vibrating diaphragm, pressure gage, planetary atmosphere, pressure measurements

REFERENCES

(1) Dimeff, J., Lane, J. W., and Coon, G. W., "New Wide Range Pressure Transducer," REVIEW OF SCIENTIFIC INSTRUMENTS, Vol. 33, 1962, p. 804.

(2) Anon., "Vibrating Diaphragm Pressure Transducer," NASA SP-5020, 1966.

(3) Zener, C., Elasticity and Anelasticity of Metals, Chicago Press, 1948.

(4) Nowick, A. S., "Internal Friction, Damping and Cyclic Plasticity," ASTM STP 378, 1965.

(5) Niblett, D. H., and Wilks, J., ADVANCES IN PHYSICS, 1960, p. 911.

(6) Sommer, S. C., Boissevain, A. G., Yee, L., and Hedlund, R. C., "The Structure of an Atmosphere From On-Board Measurements of Pressure, Temperature, and Acceleration," NASA TN D-3933, 1967.

(7) Sommer, S. C., and Yee, L., "An Experiment to Determine the Structure of a Planetary Atmosphere," AIAA 68-1054, 1968.

TABLE I. TRANSDUCER MEASUREMENTS

FACTOR	OLD VALUE	NEW VALUE	METHOD OF IMPROVEMENT
$Q^{-1} = \Delta f/f$ (MECHANICAL FILTER BANDWIDTH)	$3 \cdot 10^{-5}$	$4 \cdot 10^{-6}$	ANNEALING OF COMPLETED TRANSDUCER
LOW PRESSURE RESOLUTION	10^{-5} torr	10^{-6} torr	HIGHER DIAPHRAGM Q
HIGH PRESSURE LIMIT	$3 \cdot 10^{2}$ torr	$5 \cdot 10^{3}$ torr	GRID TYPE TRANSDUCER
FREQUENCY CHANGE WITH PRESSURE (f_0 = LOW PRESSURE RESONANT FREQUENCY)	$2 f_0$	$0.2 f_0$	GRID TYPE TRANSDUCER
SENSITIVITY TO J_{02} BESSEL MODE	$10^{-2} J_{01}$	$2 \cdot 10^{-5} J_{01}$	ADJUSTMENT OF DRIVE AND SENSE PLATE DIAMETERS, CONCENTRICITY AND PARALLELNESS
SENSITIVITY TO J_{21} BESSEL MODE	$10^{-3} J_{01}$	$10^{-4} J_{01}$	ADJUSTMENT OF DRIVE AND SENSE PLATE SENSITIVITIES, CONCENTRICITY AND PARALLELNESS

NATIONAL AERONAUTICS AND SPACE ADMINISTRATION
AMES RESEARCH CENTER, MOFFETT FIELD, CALIFORNIA

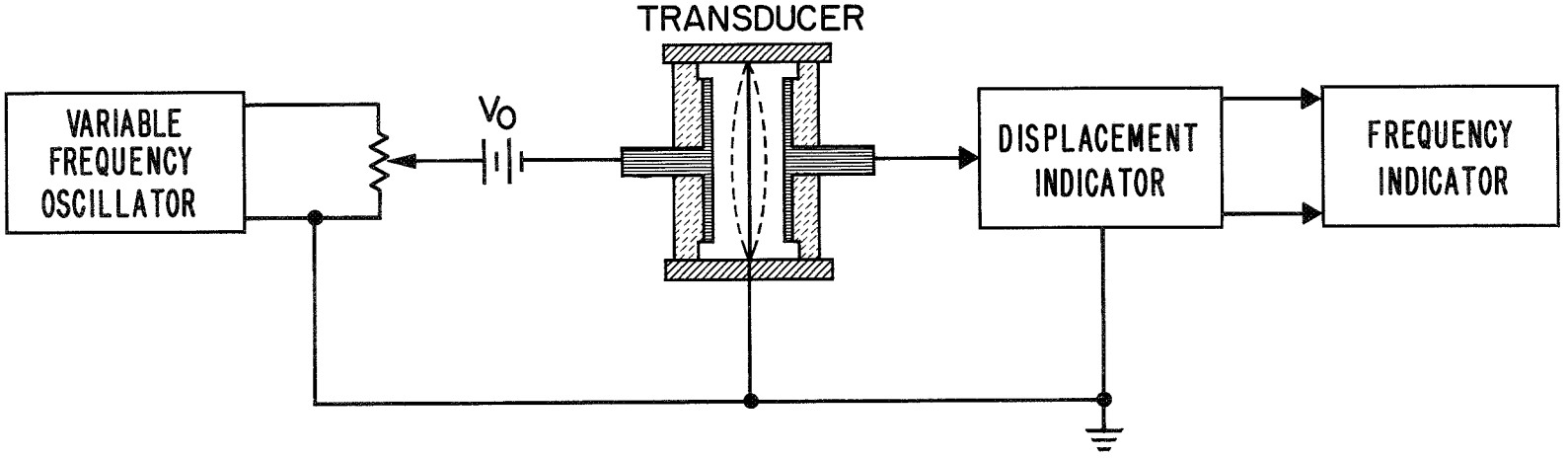

Fig. 1.- Open loop operation of the vibrating diaphragm transducer.

NATIONAL AERONAUTICS AND SPACE ADMINISTRATION
AMES RESEARCH CENTER, MOFFETT FIELD, CALIFORNIA

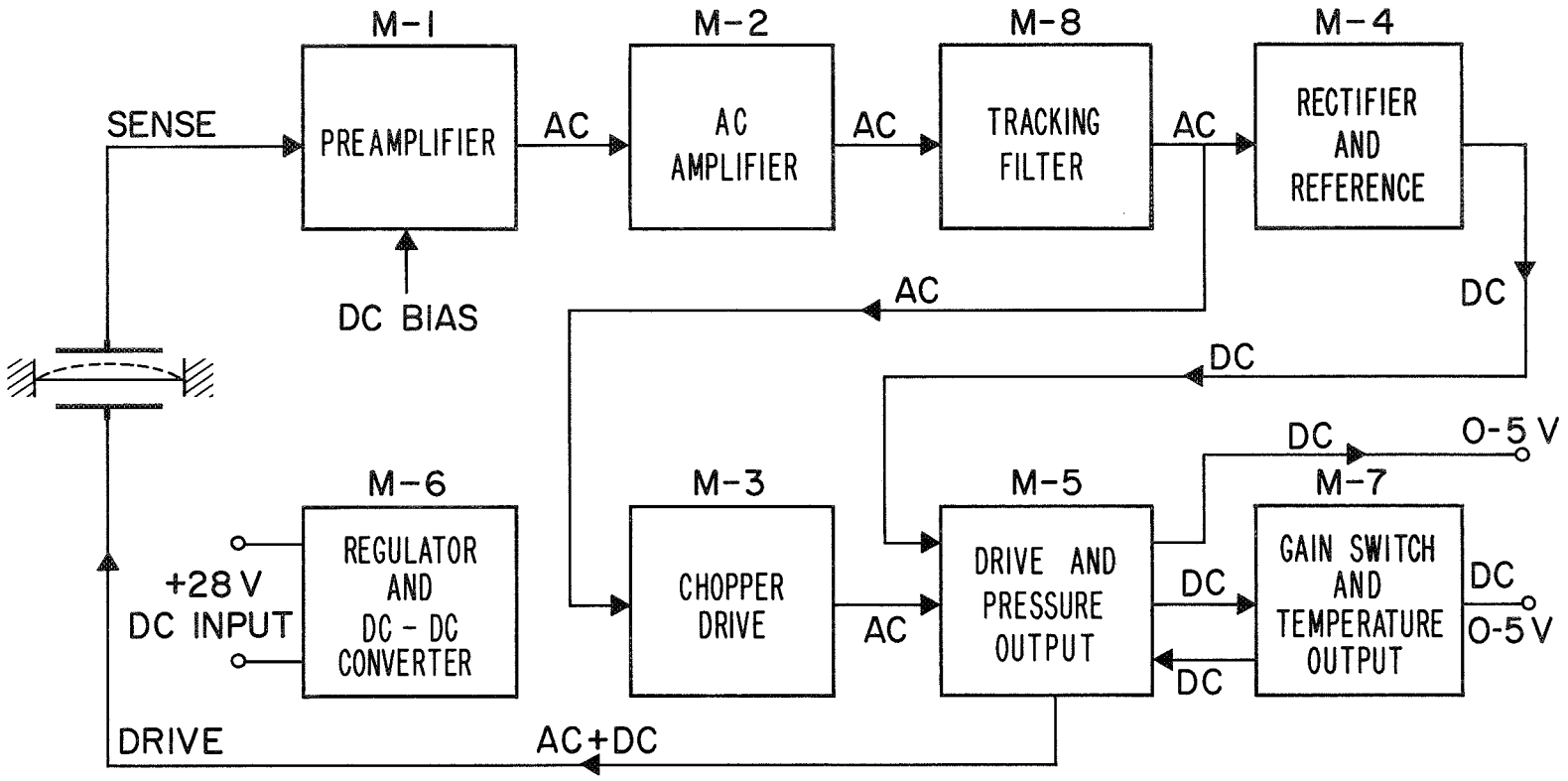

Fig. 2.- Block diagram for the vibrating diaphragm system.

NATIONAL AERONAUTICS AND SPACE ADMINISTRATION
AMES RESEARCH CENTER, MOFFETT FIELD, CALIFORNIA

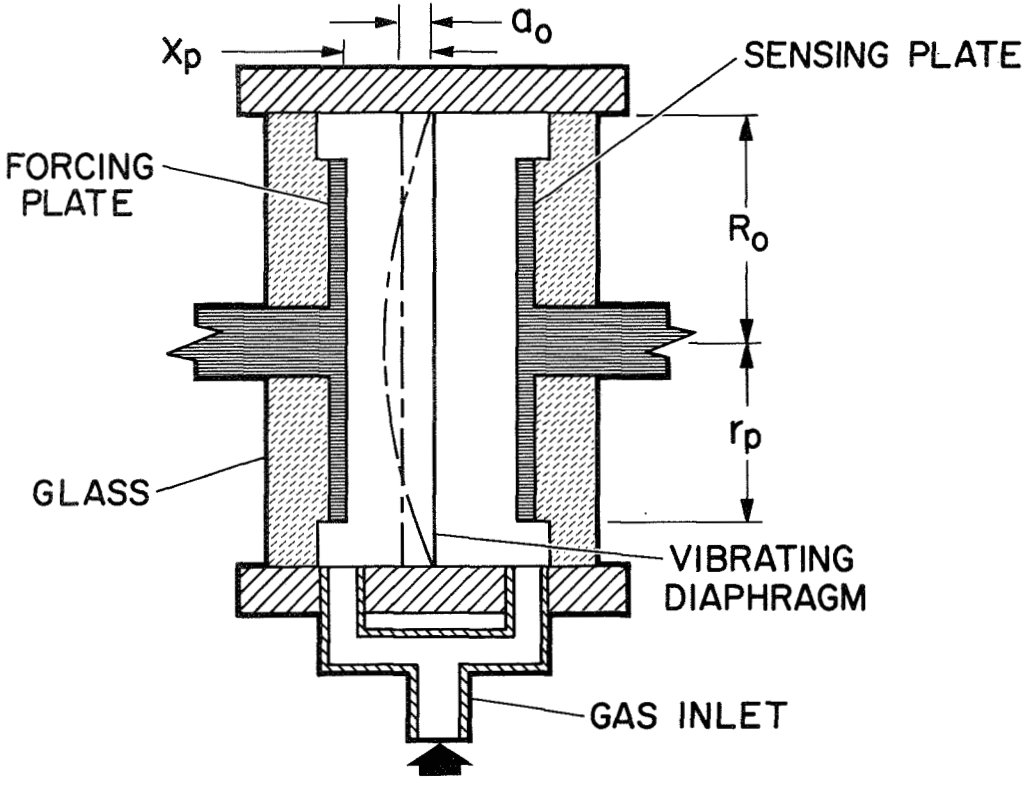

$R_o = 8.3 \times 10^{-3}$ m
$r_p = 7 \times 10^{-3}$ m
$X_p = 7.5 \times 10^{-5}$ m
$a_o = 7.5 \times 10^{-10}$ m
$t = 2.5 \times 10^{-6}$ m
$\omega_o = 3.6 \times 10^4$ rad/sec
$Q = 3 \times 10^4$
$Q = 2\pi \frac{W}{\Delta W}$

Fig. 3.- Simplified sketch of the original embodiment.

SCHEMATIC REPRESENTATION OF GRID-TYPE TRANSDUCER HALF

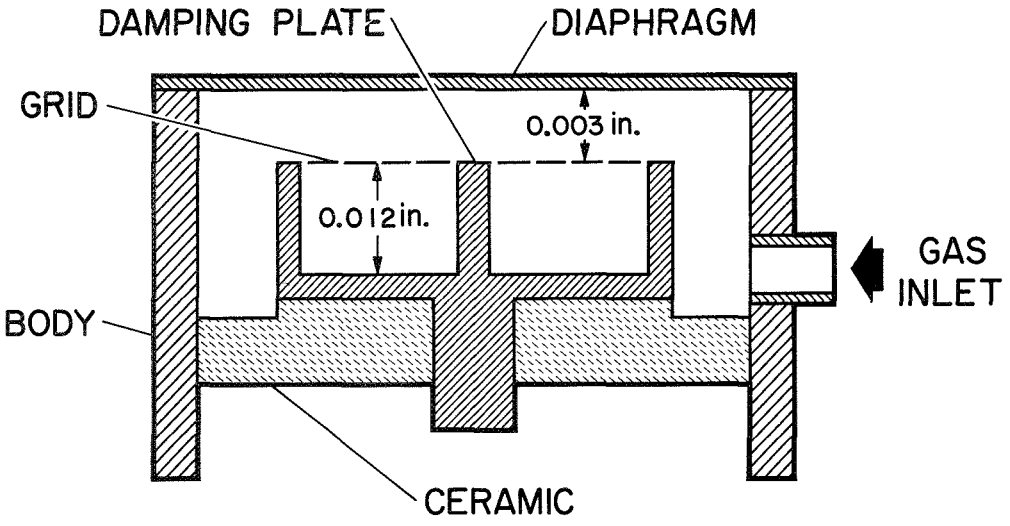

SIMPLIFIED SKETCH OF DAMPING PLATE

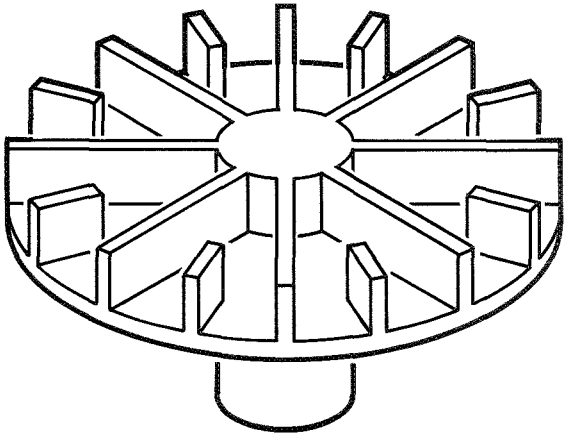

Fig. 4.- Grid-type pressure transducer.

NATIONAL AERONAUTICS AND SPACE ADMINISTRATION
AMES RESEARCH CENTER, MOFFETT FIELD, CALIFORNIA

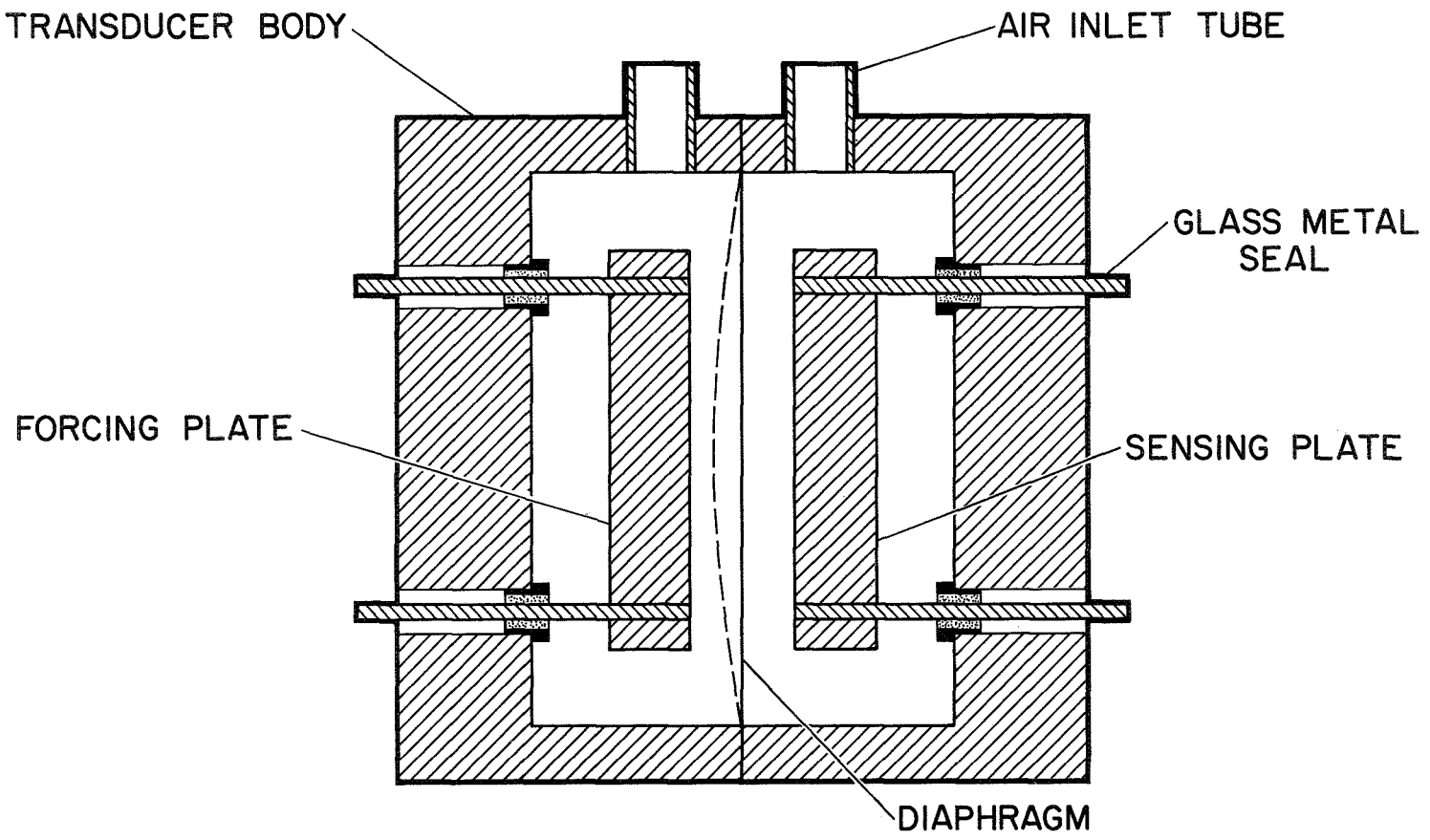

Fig. 5.- Sketch for transducer utilizing small seals.

NATIONAL AERONAUTICS AND SPACE ADMINISTRATION
AMES RESEARCH CENTER, MOFFETT FIELD, CALIFORNIA

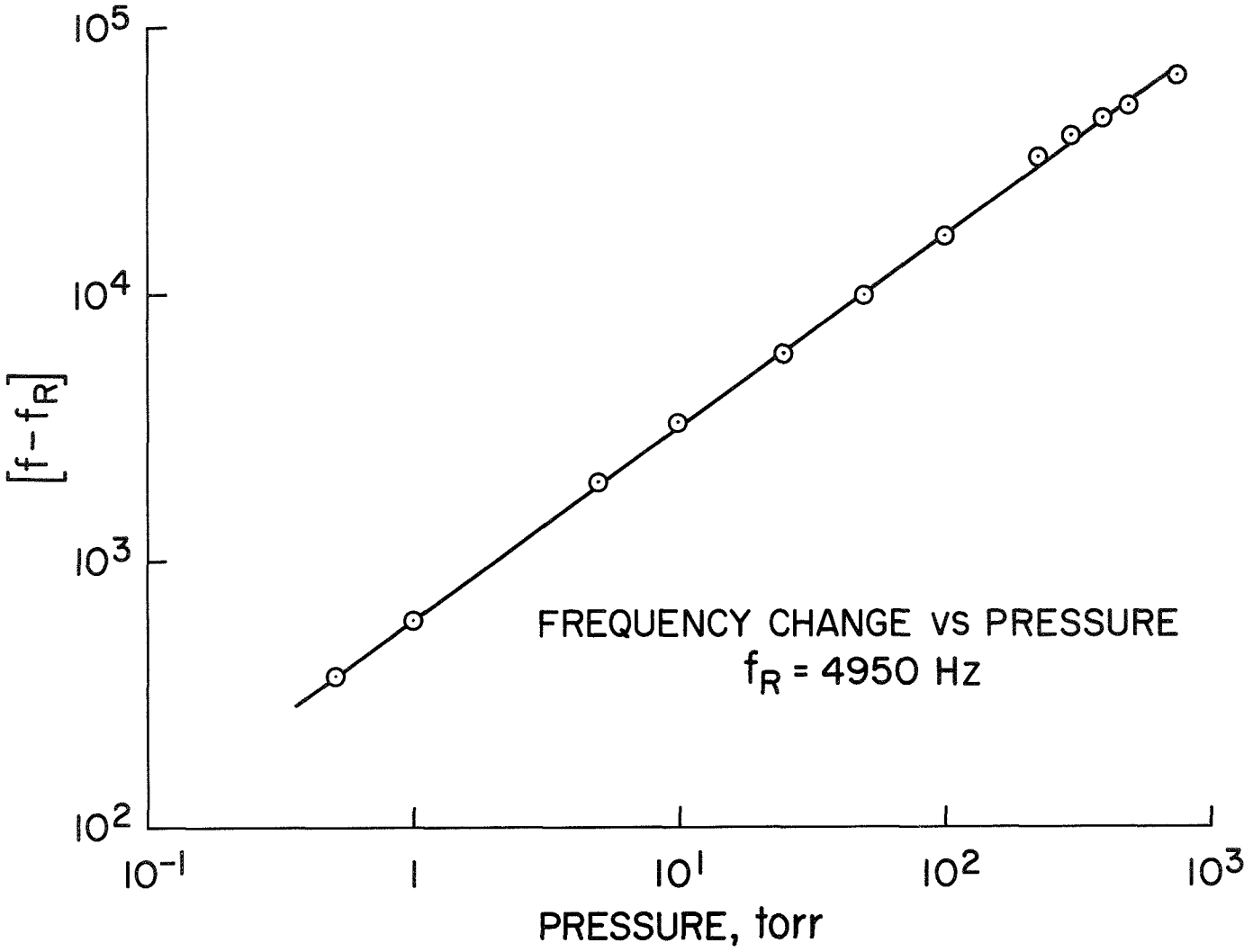

Fig. 6.- Pressure calibration for the new transducer design.

NATIONAL AERONAUTICS AND SPACE ADMINISTRATION
AMES RESEARCH CENTER, MOFFETT FIELD, CALIFORNIA

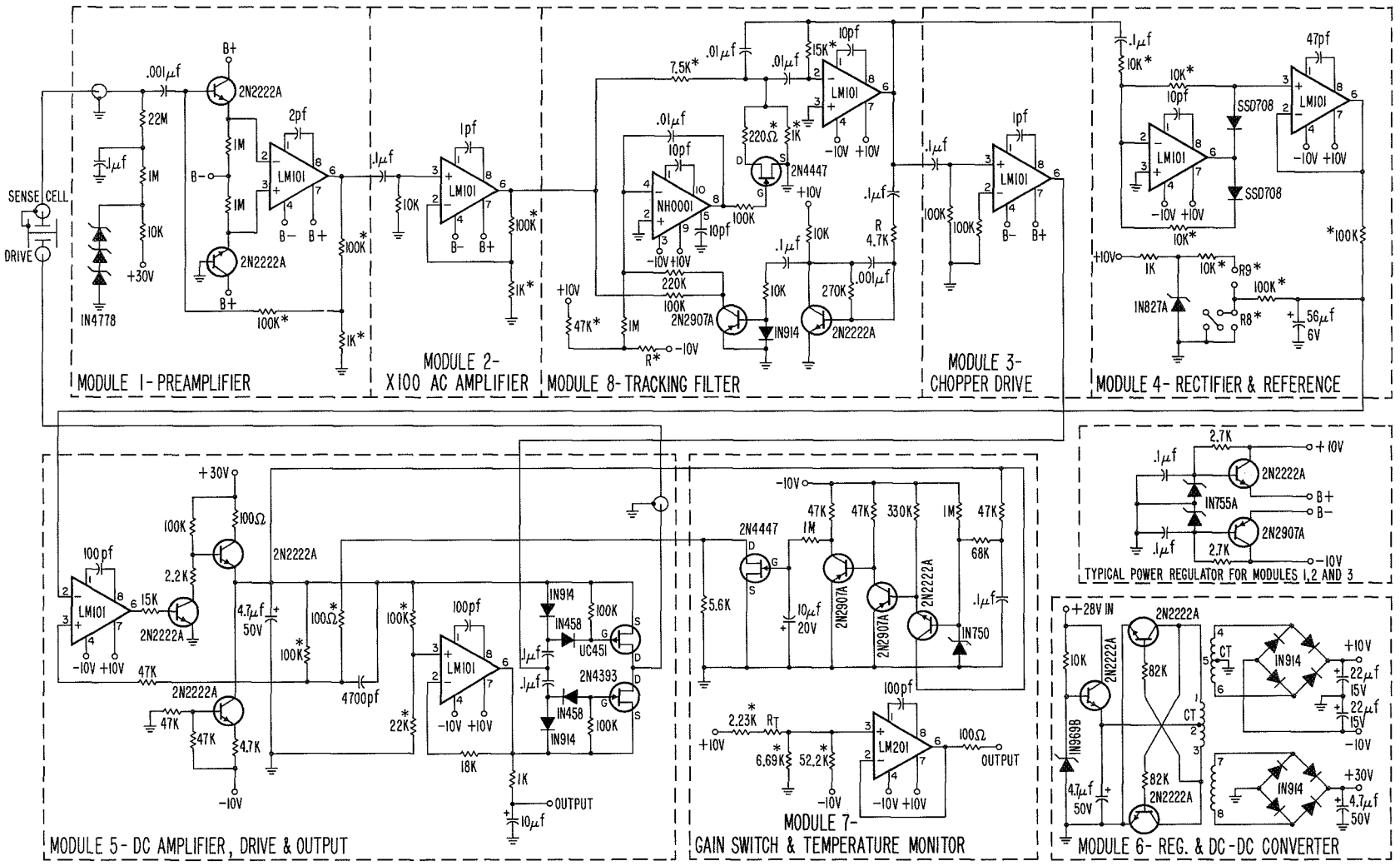

Fig. 7.- Vibrating diaphragm pressure cell electronics system.

NATIONAL AERONAUTICS AND SPACE ADMINISTRATION
AMES RESEARCH CENTER, MOFFETT FIELD, CALIFORNIA

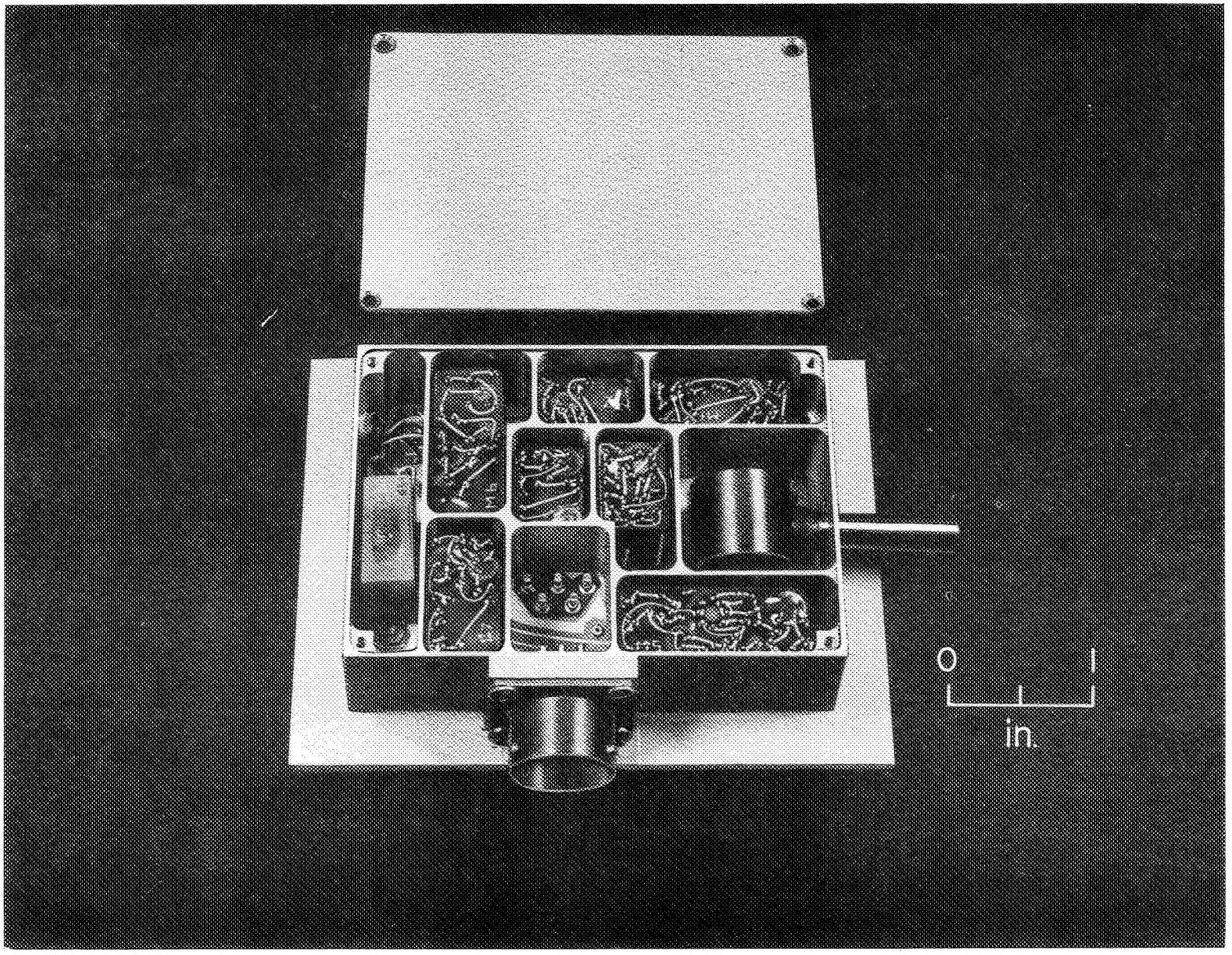

Fig. 8.- Vibrating diaphragm pressure measuring system.

NATIONAL AERONAUTICS AND SPACE ADMINISTRATION
AMES RESEARCH CENTER, MOFFETT FIELD, CALIFORNIA

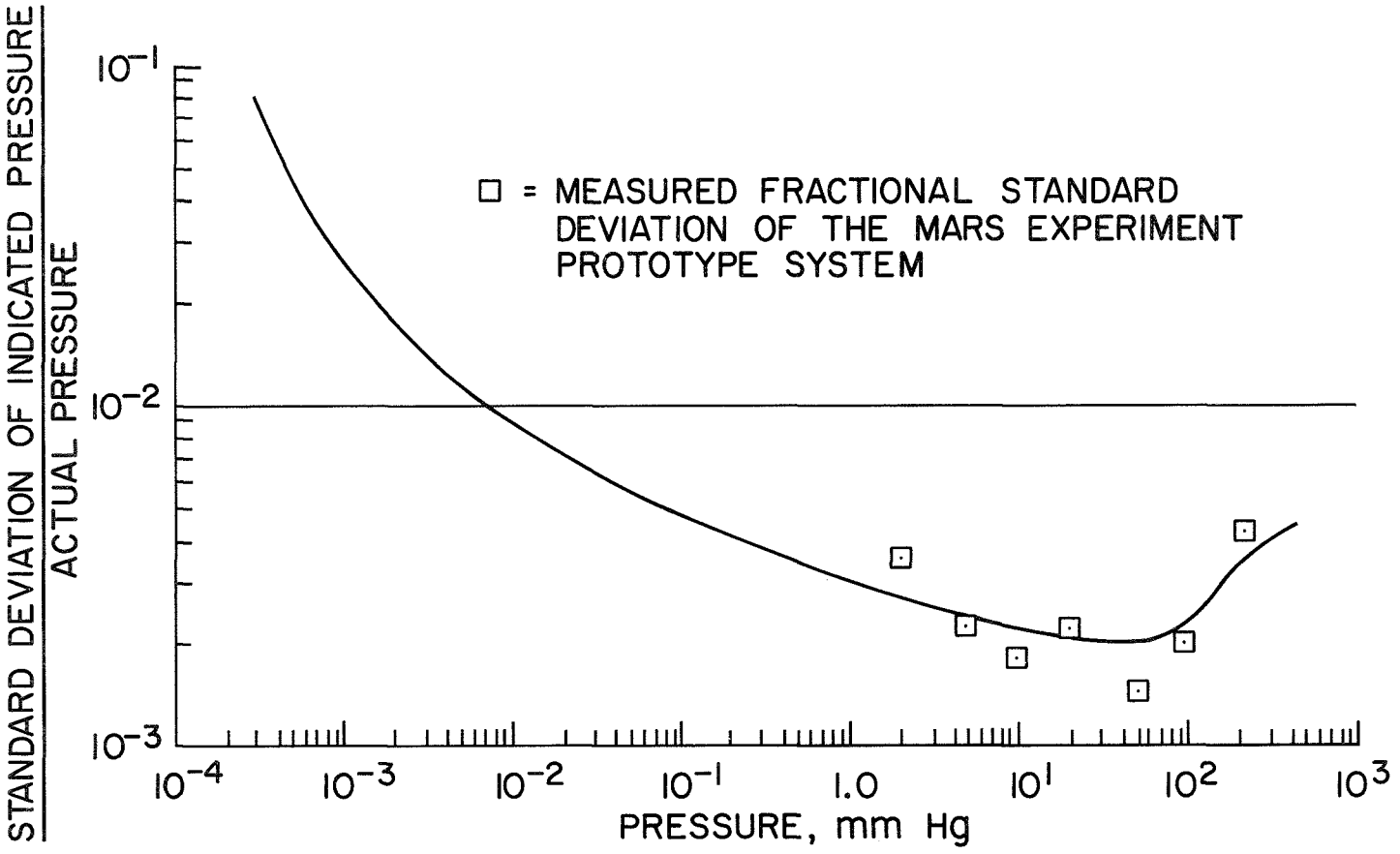

Fig. 9.- Pressure indication stability of vibrating diaphragm transducer as a function of pressure.

NATIONAL AERONAUTICS AND SPACE ADMINISTRATION
AMES RESEARCH CENTER, MOFFETT FIELD, CALIFORNIA

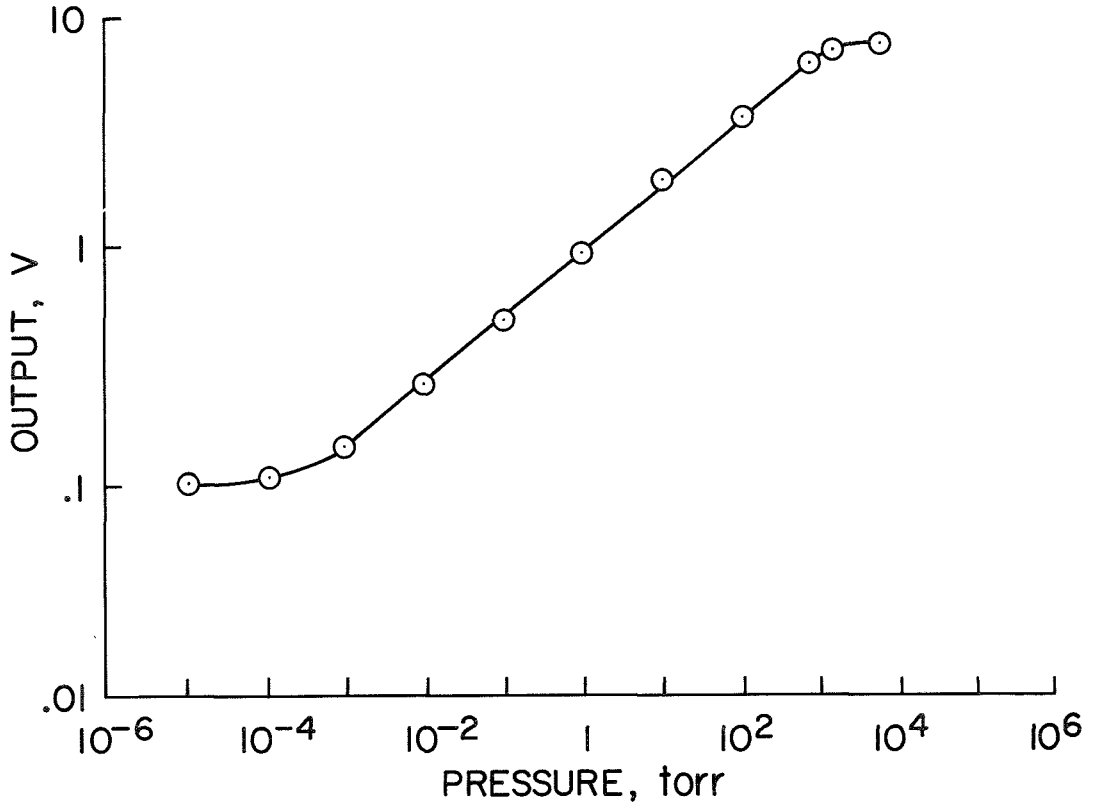

Fig. 10.- Measured preformance of vibrating diaphragm pressure cell system.

NATIONAL AERONAUTICS AND SPACE ADMINISTRATION
AMES RESEARCH CENTER, MOFFETT FIELD, CALIFORNIA